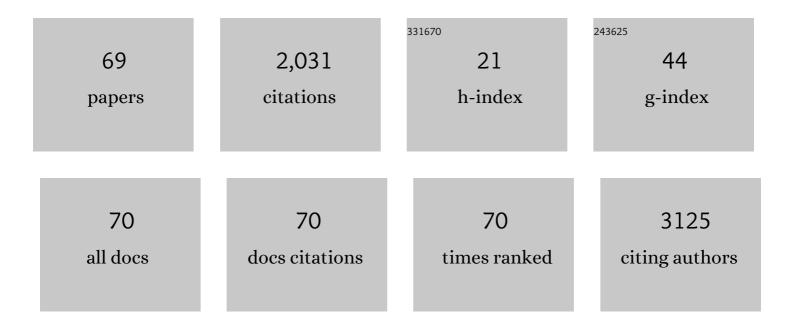
List of Publications by Year in descending order

Source: https://exaly.com/author-pdf/2015881/publications.pdf Version: 2024-02-01



FUL GIRSON

#	Article	IF	CITATIONS
1	Artificial Intelligence with Statistical Confidence Scores for Detection of Acute or Subacute Hemorrhage on Noncontrast CT Head Scans. Radiology: Artificial Intelligence, 2022, 4, .	5.8	9
2	No Surprises: Training Robust Lung Nodule Detection for Low-Dose CT Scans by Augmenting With Adversarial Attacks. IEEE Transactions on Medical Imaging, 2021, 40, 335-345.	8.9	26
3	Quantifying and leveraging predictive uncertainty for medical image assessment. Medical Image Analysis, 2021, 68, 101855.	11.6	28
4	Stochastic Sequential Modeling: Toward Improved Prostate Cancer Diagnosis Through Temporal-Ultrasound. Annals of Biomedical Engineering, 2021, 49, 573-584.	2.5	0
5	Evaluating deep learning methods in detecting and segmenting different sizes of brain metastases on 3D post-contrast T1-weighted images. Journal of Medical Imaging, 2021, 8, 037001.	1.5	9
6	GAMER MRI: Gated-attention mechanism ranking of multi-contrast MRI in brain pathology. NeuroImage: Clinical, 2021, 29, 102522.	2.7	4
7	Validation of a fully automated liver segmentation algorithm using multi-scale deep reinforcement learning and comparison versus manual segmentation. European Journal of Radiology, 2020, 126, 108918.	2.6	31
8	Class-Aware Adversarial Lung Nodule Synthesis In CT Images. , 2019, , .		16
9	Automatic segmentation of prostate MRI using convolutional neural networks: Investigating the impact of network architecture on the accuracy of volume measurement and MRI-ultrasound registration. Medical Image Analysis, 2019, 58, 101558.	11.6	45
10	Quantifying and Leveraging Classification Uncertainty for Chest Radiograph Assessment. Lecture Notes in Computer Science, 2019, , 676-684.	1.3	21
11	Conditional Segmentation in Lieu of Image Registration. Lecture Notes in Computer Science, 2019, , 401-409.	1.3	8
12	A self-tuned graph-based framework for localization and grading prostate cancer lesions: An initial evaluation based on multiparametric magnetic resonance imaging. Computers in Biology and Medicine, 2018, 96, 252-265.	7.0	3
13	NiftyNet: a deep-learning platform for medical imaging. Computer Methods and Programs in Biomedicine, 2018, 158, 113-122.	4.7	407
14	Automatic Multi-Organ Segmentation on Abdominal CT With Dense V-Networks. IEEE Transactions on Medical Imaging, 2018, 37, 1822-1834.	8.9	436
15	Stochastic Modeling of Temporal Enhanced Ultrasound: Impact of Temporal Properties on Prostate Cancer Characterization. IEEE Transactions on Biomedical Engineering, 2018, 65, 1798-1809.	4.2	4
16	Determination of optimal ultrasound planes for the initialisation of image registration during endoscopic ultrasound-guided procedures. International Journal of Computer Assisted Radiology and Surgery, 2018, 13, 875-883.	2.8	6
17	The semiotics of medical image Segmentation. Medical Image Analysis, 2018, 44, 54-71.	11.6	20
18	Adversarial Deformation Regularization for Training Image Registration Neural Networks. Lecture Notes in Computer Science, 2018, , 774-782.	1.3	42

#	Article	IF	CITATIONS
19	Inter-site Variability in Prostate Segmentation Accuracy Using Deep Learning. Lecture Notes in Computer Science, 2018, , 506-514.	1.3	37
20	Prostate lesion delineation from multiparametric magnetic resonance imaging based on locality alignment discriminant analysis. Medical Physics, 2018, 45, 4607-4618.	3.0	6
21	Weakly-supervised convolutional neural networks for multimodal image registration. Medical Image Analysis, 2018, 49, 1-13.	11.6	280
22	Integration of spatial information in convolutional neural networks for automatic segmentation of intraoperative transrectal ultrasound images. Journal of Medical Imaging, 2018, 6, 1.	1.5	23
23	Development of a computer aided diagnosis model for prostate cancer classification on multi-parametric MRI. , 2018, , .		1
24	Deep residual networks for automatic segmentation of laparoscopic videos of the liver. Proceedings of SPIE, 2017, , .	0.8	15
25	Beam distortion due to gold fiducial markers during salvage highâ€intensity focused ultrasound in the prostate. Medical Physics, 2017, 44, 679-693.	3.0	8
26	Prostate lesion detection and localization based on locality alignment discriminant analysis. Proceedings of SPIE, 2017, , .	0.8	3
27	Models of temporal enhanced ultrasound data for prostate cancer diagnosis: the impact of time-series order. , 2017, , .		0
28	Intraoperative Organ Motion Models with an Ensemble of Conditional Generative Adversarial Networks. Lecture Notes in Computer Science, 2017, , 368-376.	1.3	8
29	Towards Image-Guided Pancreas and Biliary Endoscopy: Automatic Multi-organ Segmentation on Abdominal CT with Dense Dilated Networks. Lecture Notes in Computer Science, 2017, , 728-736.	1.3	28
30	Designing image segmentation studies: Statistical power, sample size and reference standard quality. Medical Image Analysis, 2017, 42, 44-59.	11.6	12
31	MP70-02 CORRELATION OF MPMRI CONTOURS WITH 3-DIMENSIONAL 5MM TRANSPERINEAL PROSTATE MAPPING BIOPSY WITHIN THE PROMIS TRIAL PILOT: WHAT MARGINS ARE REQUIRED?. Journal of Urology, 2017, 197, .	0.4	0
32	MP38-07 SHOULD WE AIM FOR THE CENTRE OF AN MRI PROSTATE LESION? CORRELATION BETWEEN MPMRI AND 3-DIMENSIONAL 5MM TRANSPERINEAL PROSTATE MAPPING BIOPSIES FROM THE PROMIS TRIAL. Journal of Urology, 2017, 197, .	0.4	2
33	Toward Prostate Cancer Contouring Guidelines on Magnetic Resonance Imaging: Dominant Lesion Gross and Clinical Target Volume Coverage Via Accurate Histology Fusion. International Journal of Radiation Oncology Biology Physics, 2016, 96, 188-196.	0.8	26
34	Determination of the Association Between T2-weighted MRI and Gleason Sub-pattern: A Proof of Principle Study. Academic Radiology, 2016, 23, 1412-1421.	2.5	19
35	Fusion of multi-parametric MRI and temporal ultrasound for characterization of prostate cancer: in vivo feasibility study. , 2016, , .		3
36	Classification of prostate cancer grade using temporal ultrasound: in vivo feasibility study. Proceedings of SPIE, 2016, , .	0.8	0

#	Article	IF	CITATIONS
37	How does prostate biopsy guidance error impact pathologic cancer risk assessment?. , 2016, , .		0
38	Prostate Cancer: Improved Tissue Characterization by Temporal Modeling of Radio-Frequency Ultrasound Echo Data. Lecture Notes in Computer Science, 2016, , 644-652.	1.3	3
39	A Method for 3D Histopathology Reconstruction Supporting Mouse Microvasculature Analysis. PLoS ONE, 2015, 10, e0126817.	2.5	28
40	Using Hidden Markov Models to capture temporal aspects of ultrasound data in prostate cancer. , 2015, , .		9
41	Ultrasound-Based Characterization of Prostate Cancer Using Joint Independent Component Analysis. IEEE Transactions on Biomedical Engineering, 2015, 62, 1796-1804.	4.2	14
42	Computer-Aided Prostate Cancer Detection Using Ultrasound RF Time Series: In Vivo Feasibility Study. IEEE Transactions on Medical Imaging, 2015, 34, 2248-2257.	8.9	37
43	Population-based prediction of subject-specific prostate deformation for MR-to-ultrasound image registration. Medical Image Analysis, 2015, 26, 332-344.	11.6	33
44	Statistical Power in Image Segmentation: Relating Sample Size to Reference Standard Quality. Lecture Notes in Computer Science, 2015, , 105-113.	1.3	0
45	Spatially varying accuracy and reproducibility of prostate segmentation in magnetic resonance images using manual and semiautomated methods. Medical Physics, 2014, 41, 113503.	3.0	16
46	Multiparametric MR imaging of prostate cancer foci: assessing the detectability and localizability of Gleason 7 peripheral zone cancers based on image contrasts. , 2014, , .		1
47	3D reconstruction of digitized histological sections for vasculature quantification in the mouse hind limb. Proceedings of SPIE, 2014, , .	0.8	1
48	Accuracy and variability of tumor burden measurement on multi-parametric MRI. , 2014, , .		0
49	A dimensionless dynamic contrast enhanced MRI parameter for intra-prostatic tumour target volume delineation: initial comparison with histology. , 2014, , .		0
50	The impact of registration accuracy on imaging validation study design: A novel statistical power calculation. Medical Image Analysis, 2013, 17, 805-815.	11.6	11
51	Toward quantitative digital histopathology for prostate cancer: comparison of inter-slide interpolation methods for tumour measurement. Proceedings of SPIE, 2013, , .	0.8	3
52	3D prostate histology reconstruction: an evaluation of image-based and fiducial-based algorithms. Proceedings of SPIE, 2013, , .	0.8	1
53	3D prostate histology image reconstruction: Quantifying the impact of tissue deformation and histology section location. Journal of Pathology Informatics, 2013, 4, 31.	1.7	29
54	Ultrasound-Based Characterization of Prostate Cancer: An in vivo Clinical Feasibility Study. Lecture Notes in Computer Science, 2013, 16, 279-286.	1.3	7

#	Article	IF	CITATIONS
55	Prostate: Registration of Digital Histopathologic Images to in Vivo MR Images Acquired by Using Endorectal Receive Coil. Radiology, 2012, 263, 856-864.	7.3	62
56	3D reconstruction of prostate histology based on quantified tissue cutting and deformation parameters. Proceedings of SPIE, 2012, , .	0.8	5
57	Registration of prostate histology images to ex vivo MR images via strandâ€shaped fiducials. Journal of Magnetic Resonance Imaging, 2012, 36, 1402-1412.	3.4	58
58	Registration Accuracy: How Good Is Good Enough? A Statistical Power Calculation Incorporating Image Registration Uncertainty. Lecture Notes in Computer Science, 2012, 15, 643-650.	1.3	6
59	Co-registration Framework for Histology-registration-based Validation of Fused Multimodality Prostate Cancer Imaging. , 2011, , .		0
60	189 REGISTRATION OF DIGITAL HISTOLOGY IMAGES TO IN VIVO MRI FOR PROSTATE CANCER FOCAL THERAPY RESEARCH. Journal of Urology, 2011, 185, .	0.4	0
61	Tissue block MRI for slice orientation-independent registration of digital histology images to ex vivo MRI of the prostate. , 2011, , .		4
62	A semi-automated method for identifying and measuring myelinated nerve fibers in scanning electron microscope images. Journal of Neuroscience Methods, 2011, 201, 149-158.	2.5	50
63	Image-guided prostate sectioning supporting registration of graded cancerous foci from digital histopathology images to in vivo MRI: an interactive 3D visualization tool. , 2011, , .		1
64	Validation of Direct Registration of Whole-Mount Prostate Digital Histopathology to ex vivo MR Images. Lecture Notes in Computer Science, 2011, , 134-145.	1.3	5
65	Morphometric analysis of the optic nerve head with optical coherence tomography. Proceedings of SPIE, 2010, , .	0.8	2
66	Longitudinal study of retinal degeneration in a rat using spectral domain optical coherence tomography. Optics Express, 2010, 18, 23435.	3.4	23
67	Optic Nerve Head Registration Via Hemispherical Surface and Volume Registration. IEEE Transactions on Biomedical Engineering, 2010, 57, 2592-2595.	4.2	13
68	Registration of In Vivo Prostate Magnetic Resonance Images to Digital Histopathology Images. Lecture Notes in Computer Science, 2010, , 66-76.	1.3	16
69	A Combined Surface And VOlumetric Registration (SAVOR) Framework to Study Cortical Biomarkers and Volumetric Imaging Data. Lecture Notes in Computer Science, 2009, 12, 713-720.	1.3	3